

# NASA TECHNICAL MEMORANDUM

NASA TM X-72687

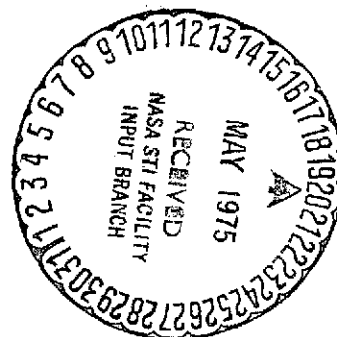
NASA TM X-72687

(NASA-TM-X-72687) ULTRASONIC DISPLACEMENT  
SYSTEM (NASA) 15 P HC \$3.25 CACL 20A

N75-23245

Unclas  
G3/71 19460

ULTRASONIC DISPLACEMENT SYSTEM



By Nettie D. Faulcon

This informal documentation medium is used to provide accelerated or special release of technical information to selected users. The contents may not meet NASA formal editing and publication standards, may be revised, or may be incorporated in another publication.

NATIONAL AERONAUTICS AND SPACE ADMINISTRATION  
LANGLEY RESEARCH CENTER, HAMPTON, VIRGINIA 23665

1. Report No. TM X-72687		2. Government Accession No.		3. Recipient's Catalog No.	
4. Title and Subtitle Ultrasonic Displacement System				5. Report Date April 21, 1975	
				6. Performing Organization Code	
7. Author(s) Nettie D. Faulcon				8. Performing Organization Report No.	
9. Performing Organization Name and Address NASA Langley Research Center Hampton, Virginia 23665				10. Work Unit No. 506-17-31-02	
				11. Contract or Grant No.	
12. Sponsoring Agency Name and Address National Aeronautics and Space Administration Washington, DC 20546				13. Type of Report and Period Covered Technical Memorandum	
				14. Sponsoring Agency Code	
15. Supplementary Notes					
16. Abstract  In this report, an acoustic instrument system is described as a feasible tool for remote measurement of structural velocities. The system involves measurement of the doppler shift of ultrasonic sound as it is reflected from an oscillating plate. Measurements were performed in air with an ultrasonic frequency source of 42.5 kilohertz. The surface under investigation was a plexiglass plate oscillating sinusoidally at 10, 13, and 15 Hz. Data are presented to show that, in such a system, the measurement of the doppler shift is dependent upon the acoustic pathlength between the sensing device and the oscillating surface, with the distance between maximum shifts being half the wavelength of the ultrasonic source.					
17. Key Words (Suggested by Author(s)) (STAR category underlined) Ultrasonic Displacement FM Demodulation Doppler Frequency Shift				18. Distribution Statement Unclassified - Unlimited Star Category 32	
19. Security Classif. (of this report) Unclassified		20. Security Classif. (of this page) Unclassified		21. No. of Pages 13	
				22. Price* \$3.25	

\*Available from { The National Technical Information Service, Springfield, Virginia 22151  
STIF/NASA Scientific and Technical Information Facility, P.O. Box 33, College Park, MD 20740

## ULTRASONIC DISPLACEMENT SYSTEM

By Nettie D. Faulcon  
Langley Research Center

### SUMMARY

In this report, an acoustic instrument system is described as a feasible tool for remote measurement of structural velocities. The system involves measurement of the doppler shift of ultrasonic sound as it is reflected from an oscillating plate. Measurements were performed in air with an ultrasonic frequency source of 42.5 kilohertz. The surface under investigation was a plexiglass plate oscillating sinusoidally at 10, 13, and 15 Hz. Data are presented to show that, in such a system, the measurement of the doppler shift is dependent upon the acoustic pathlength between the sensing device and the oscillating surface, with the distance between maximum shifts being half the wavelength of the ultrasonic source.

### INTRODUCTION

In general, there are many proximity sensors available for measurement of structural velocities; however, these sensors are limited by such constraints as conductivity, reflectivity, level of response, and interference with the surface under investigation. In view of this, an acoustic technique was conceived as a relatively simple approach which would relax most of these constraints and additionally, allow operation in hostile environments. The technique involved sensing an ultrasonic wave doppler shifted from a vibrating surface and analyzing this reflected wave by FM demodulation. Since acoustic reflection is not dependent on conductivity or other properties of a surface,

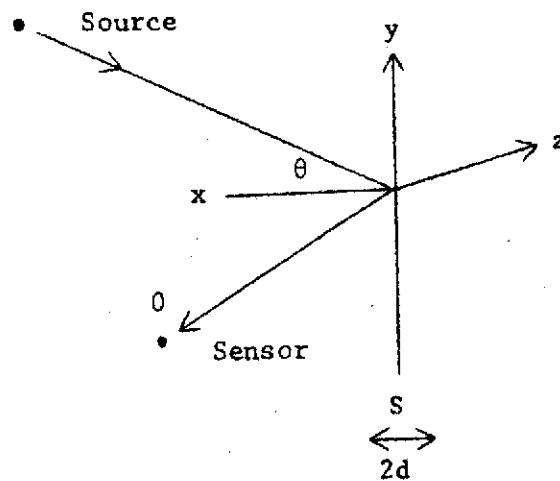
unless in absorbing medium, this technique would be useful for most surfaces. The main purpose of this report is to show that in a system with an oscillating velocity, as opposed to a constant velocity, the doppler frequency shift is dependent on the receiver to panel distance; therefore precaution should be taken for optimum location of the receiver.

#### SYMBOLS

$A_1$	amplitude of incident sound, newton/meter <sup>2</sup>
$\hat{A}_2$	complex amplitude of reflected sound, newton/meter <sup>2</sup>
$c$	speed of sound, 343 meters/second
$d$	peak amplitude of oscillating plate, meter
$K$	wave number of incident sound, meter <sup>-1</sup>
$K_1$	wave number in x-space
$K_2$	wave number in y-space
$P_i$	pressure of incident wave, newton/meter <sup>2</sup>
$P_r$	pressure of reflected wave, newton/meter <sup>2</sup>
$U_i$	particle velocity of incident wave, meter/sec
$U_r$	particle velocity of reflected wave, meter/sec
$U_s$	surface velocity of oscillating plate, meter/sec
$x_o$	position of microphone, meter
$x_s$	surface motion of oscillating plate, meter
$\theta$	angle between incident sound and receiver axis
$\lambda$	ultrasonic source wavelength, meter
$\rho$	density of air, 1.21 kilograms/meter <sup>3</sup>
$\omega$	angular frequency of incident sound, kilohertz
$\omega_s$	angular frequency of oscillating plate, hertz

## THEORY

The remote displacement sensor depends upon reflected sound for its operation. The relationship between the reflected sound and the velocity is given in the doppler theory. The following analysis gives the relationship of the wave reflected from the oscillating plate and its interaction with the incident wave:



### Assumptions:

1. Source is many wavelengths away from surface S.
2. S is infinite in extent and perfectly rigid.
3. Incident wave is plane and in the x-y plane.
4. Surface S oscillates simple harmonically in the direction of x.

Let x-y plane of the x-y-z frame of reference coincide with surface S at  $t = 0$ .

Since the medium is at rest, the incident and reflected waves for  $x > 0$  space may be written as (ref. 1)

$$\left. \begin{aligned} P_i &= A_1 \exp i(K_1 x + K_2 y - \omega t) \\ P_r &= \hat{A}_2 \exp i(-K_1 x + K_2 y - \omega t) \end{aligned} \right\} \quad (1)$$

The corresponding particle velocities are

$$\left. \begin{aligned} U_i &= \frac{K_1}{\rho c K} P_i \\ U_r &= -\frac{K_1}{\rho c K} P_r \end{aligned} \right\} \quad (2)$$

If the surface  $S$  were stationary, the boundary condition would be

$$U_i \Big|_{\text{Surface}} + U_r \Big|_{\text{Surface}} = 0 \quad (3)$$

Since the surface is oscillating, the right-hand side of equation (3) is no longer zero. Denote the surface motion by

$$x_s = d \exp i(-\omega_s t)$$

The surface velocity is then

$$U_s = \frac{dx_s}{dt} = -i\omega_s x_s \quad (4)$$

To a fixed observer, the boundary condition is

$$U_i \Big|_{\text{Surface}} + U_r \Big|_{\text{Surface}} = U_s \quad (5)$$

Assume that the surface oscillates in the  $x$  direction only,

$x = x_s = d \exp i(-\omega_s t)$  is the only equation giving the location of the surface with respect to a fixed observer. Applying the boundary condition, equation (5), one gets

$$\frac{K_1}{\rho c K} \left[ A_1 \exp i(K_1 x_s) - \hat{A}_2 \exp i(-K_1 x_s) \right] \exp i(K_2 y - \omega t) = -i\omega_s x_s \quad (6)$$

Since  $A_1$  is given, one can solve for  $\hat{A}_2$  in equation (6),

$$\hat{A}_2 = \left[ i\omega_s x_s \frac{\rho c K}{K_1} \exp i(-K_2 y + \omega t) + A_1 \exp i(K_1 x_s) \right] \exp i(K_1 x_s) \quad (7)$$

The pressure observed at the observation point is the sum of the incident wave and the reflected wave. If the position of O is given by  $(X_o, Y_o)$  with respect to the fixed coordinate (or the equilibrium position of S), then

$$\begin{aligned} P_o &= P_i|_O + P_r|_O \\ &= A_1 \exp i(K_1 X_o + K_2 Y_o - \omega t) + \hat{A}_2 \exp i(-K_1 X_o + K_2 Y_o - \omega t) \end{aligned}$$

Applying equation (7) for  $\hat{A}_2$ , one gets

$$\begin{aligned} P_o &= A_1 \exp i(K_1 X_o + K_2 Y_o - \omega t) + i\omega_s x_s \frac{\rho c K}{K_1} \exp i(-K_1 X_o + K_1 x_s) \\ &\quad + A_1 \exp i(2K_1 x_s - K_1 X_o + K_2 Y_o - \omega t) \end{aligned} \quad (8)$$

or

$$\begin{aligned} P_o &= A_1 \exp i(-\omega t) \left[ \exp i(K_1 X_o + K_2 Y_o) + \exp i(2K_1 x_s - K_1 X_o + K_2 Y_o) \right] \\ &\quad + i\omega_s x_s \frac{\rho c K}{K_1} \exp i(K_1 x_s - K_1 X_o) \end{aligned} \quad (9)$$

Setting  $K = K_1$ ,  $B = \omega_s d \rho c$ ,  $A = A_1$ , and  $Y_o = 0$ , the phase,  $\phi$ , of  $P_o$  becomes

$$\phi = \tan^{-1} \left[ \frac{-2A \sin(\omega t - Kx_s) \cos(Kx_s - KX_o) + B \cos(\omega_s t + KX_o - Kx_s)}{2A \cos(\omega t - Kx_s) \cos(Kx_s - KX_o) + B \sin(\omega_s t + KX_o - Kx_s)} \right] \quad (10)$$

Differentiating  $\phi$  with respect to time gives the doppler frequency;

$$\frac{d\phi}{dt} = \frac{\left[ 2AcKU_s \cos(\omega t - \omega_s t - KX_o) \sin(Kx_s - KX_o) - 4A^2(\omega - KU_s) \cos^2(Kx_s - KX_o) \right. \\ \left. + 2Ac(\omega - KU_s) \sin(\omega t - \omega_s t - KX_o) \cos(Kx_s - KX_o) \right. \\ \left. + 2Ac(\omega_s - KU_s) \sin(\omega t - \omega_s t - KX_o) \cos(Kx_s - KX_o) - B^2(\omega_s - KU_s) \right]}{4A^2 \cos^2(Kx_s - KX_o) - 4AB \sin(\omega t - \omega_s t - KX_o) \cos(Kx_s - KX_o) + B^2} \quad (11)$$

Factoring  $\omega$ ,  $KU_s$ , and  $\omega_s$  yields;

$$\frac{d\phi}{dt} = \omega \left[ \frac{-4A^2 \cos^2(Kx_s - KX_o) + 2AB \sin(\omega t - \omega_s t - KX_o) \cos(Kx_s - KX_o)}{4A^2 \cos^2(Kx_s - KX_o) - 4AB \sin(\omega t - \omega_s t - KX_o) \cos(Kx_s - KX_o) + B^2} \right. \\ \left. + KU_s \left[ \frac{2AB \cos(\omega t - \omega_s t - KX_o) \sin(Kx_s - KX_o) + 4A^2 \cos^2(Kx_s - KX_o) - 4AB \sin(\omega t - \omega_s t - KX_o) \cos(Kx_s - KX_o) + B^2}{4A^2 \cos^2(Kx_s - KX_o) - 4AB \sin(\omega t - \omega_s t - KX_o) \cos(Kx_s - KX_o) + B^2} \right] \right. \\ \left. + \omega_s \left[ \frac{2AB \sin(\omega t - \omega_s t - KX_o) \cos(Kx_s - KX_o) - B^2}{4A^2 \cos^2(Kx_s - KX_o) - 4AB \sin(\omega t - \omega_s t - KX_o) \cos(Kx_s - KX_o) + B^2} \right] \right] \quad (12)$$



which reduces to:

$$\begin{aligned}
 \frac{d\phi}{dt} = & -\omega \left[ 1 + \frac{2AB \sin(\omega t - \omega_s t - KX_o) \cos(Kx_s - KX_o) - B^2}{4A^2 \cos^2(Kx_s - KX_o) - 4AB \sin(\omega t - \omega_s t - KX_o) \cos(Kx_s - KX_o) + B^2} \right] \\
 & + KU_s \left[ 1 + \frac{2AB \cos(\omega t - \omega_s t - KX_o) \sin(Kx_s - KX_o)}{4A^2 \cos^2(Kx_s - KX_o) - 4AB \sin(\omega t - \omega_s t - KX_o) \cos(Kx_s - KX_o) + B^2} \right] \\
 & + \omega_s \left[ \frac{2AB \sin(\omega t - \omega_s t - KX_o) \cos(Kx_s - KX_o) - B^2}{4A^2 \cos^2(Kx_s - KX_o) - 4AB \sin(\omega t - \omega_s t - KX_o) \cos(Kx_s - KX_o) + B^2} \right]
 \end{aligned} \tag{13}$$

This relationship may be alternatively written as:

$$\frac{d\phi}{dt} = -\omega + KU_s + \left\{ \frac{-(\omega - \omega_s) \left[ 2AB \sin(\omega t - \omega_s t - KX_o) \cos(Kx_s - KX_o) - B^2 \right] + KU_s \left[ 2AB \cos(\omega t - \omega_s t - KX_o) \sin(Kx_s - KX_o) \right]}{4A^2 \cos^2(Kx_s - KX_o) - 4AB \sin(\omega t - \omega_s t - KX_o) \cos(Kx_s - KX_o) + B^2} \right\} \tag{14}$$

Equation (14) shows the standard doppler equation plus an additional term which influences the doppler frequency according to observer position  $X_o$ . The frequency shift in (14) was determined ( $t = 0$ ,  $\omega = 42.5$  kHz,  $\omega_s = 10$  Hz,  $A = 10^{-4}$  m) for different observer positions,  $X_o$ . Figure 1 shows the

magnitude of the shifts as a function of  $X_0$ . It is seen in the figure that maximum magnitude values are approximately 0.004 meter apart as are the minimum values. This separation of maximum or minimum points represents half wavelengths of the 42.5 kHz source frequency in air.

#### EXPERIMENTAL SETUP AND PROCEDURE

The experimental setup used is shown in figure 2. The tests were performed in air with no specific requirement of the surrounding environment. The sound frequency and the frequency of the oscillating surface were chosen and limited only by the specifications of the equipment used.

The sound source was a ring radiator oscillating at 42.5 kHz (wavelength = 0.008 m). This frequency was chosen because it afforded no appreciable absorption in air and was convenient for the equipment used. To insure accurate frequency, a frequency generator-synthesizer was used to drive the radiator. The distribution pattern of the source was determined and its maximum axis of vibration was placed several wavelengths from the test surface, a plexiglass plate (12.7 cm by 17.8 cm). The amplitude and frequency of the test surface were controlled by regulating the corresponding parameters of the vibration exciter on which it was mounted. The reflected sound was detected by a probe system consisting of a 0.63 cm (1/4 in.) condenser microphone and a stainless-steel tube, 240 mm in length, 4 mm in diameter. The position of the probe tube in reference to the surface was read on a millimeter scale. For determination of the doppler shift, the probe output was transmitted to an FM demodulator tuned to  $42.5 \text{ kHz} \pm 2 \text{ kHz}$ . The bandwidth of  $\pm 2 \text{ kHz}$  was selected because it encompasses the doppler shift encountered

in the present study; however, if a higher shift is anticipated, a higher bandwidth could be used. The demodulator delivered a voltage output proportional to the deviation of the input signal from 42.5 kHz. For the purpose of reading and observing the shift an ac meter and an oscilloscope were used.

The sound source amplitude and the microphone response were checked to maintain at least 2 mV output, the minimum requirement necessary for satisfactory operation of the demodulator.

### EXPERIMENTAL DISCUSSION

The system was tested with the surface oscillating at 10, 13, and 15 Hz. In each test, the amplitude of the shift, as given by the demodulator output, was altered according to the amplitude and frequency of the test surface. It was found, however, that in all the tests, the shift amplitude was further dependent on the position of the probe microphone. For the same input, but different probe positions, the output varied with a pattern similar to amplitude patterns characteristic of standing waves. Figure 3 represents the rms voltage output of the demodulator, which is proportional to the frequency shift, as a function of probe position with the test surface oscillating at 10 Hz. This pattern nearly follows the pattern derived from equation (14), figure 1. In both figures the maximum shifts were located at half wavelength intervals of the ultrasonic frequency.

### CONCLUSION

An acoustic doppler shift technique for measuring structural velocities has been investigated. A system was designed and experimental application demonstrated the feasibility of using the system as a remote displacement

sensor. The sensor works independently of many of the constraints of other sensors. However, this technique has proven to be very sensitive to the position of the probe as related to the oscillating surface. The theoretical treatment developed a frequency equation which showed that the doppler frequency was influenced by a factor dependent on the position of the observer. The experimental work was concerned with the demonstration of this phenomenon and, consequently, no absolute calibrations of the frequency shifts were made. By changing the position of the microphone with respect to the surface, the distances between maximum frequency changes were determined. These distances agreed with the path lengths between the theoretically determined maximum frequency changes. It is therefore shown that optimum output can be determined from optimum receiver position. However, if one wishes to make a more accurate measurement, a sensitivity calibration at the selected microphone position will have to be made.

#### REFERENCES

1. Kinsler, L. E.; and Frey, A. R.: Fundamentals of Acoustics, John Wiley and Sons, Inc., New York, 1962.
2. Stephens, R. W. B.; and Bute, A. E.: Acoustics and Vibrational Physics, Edward Arnold, L.T.D., London, 1966.

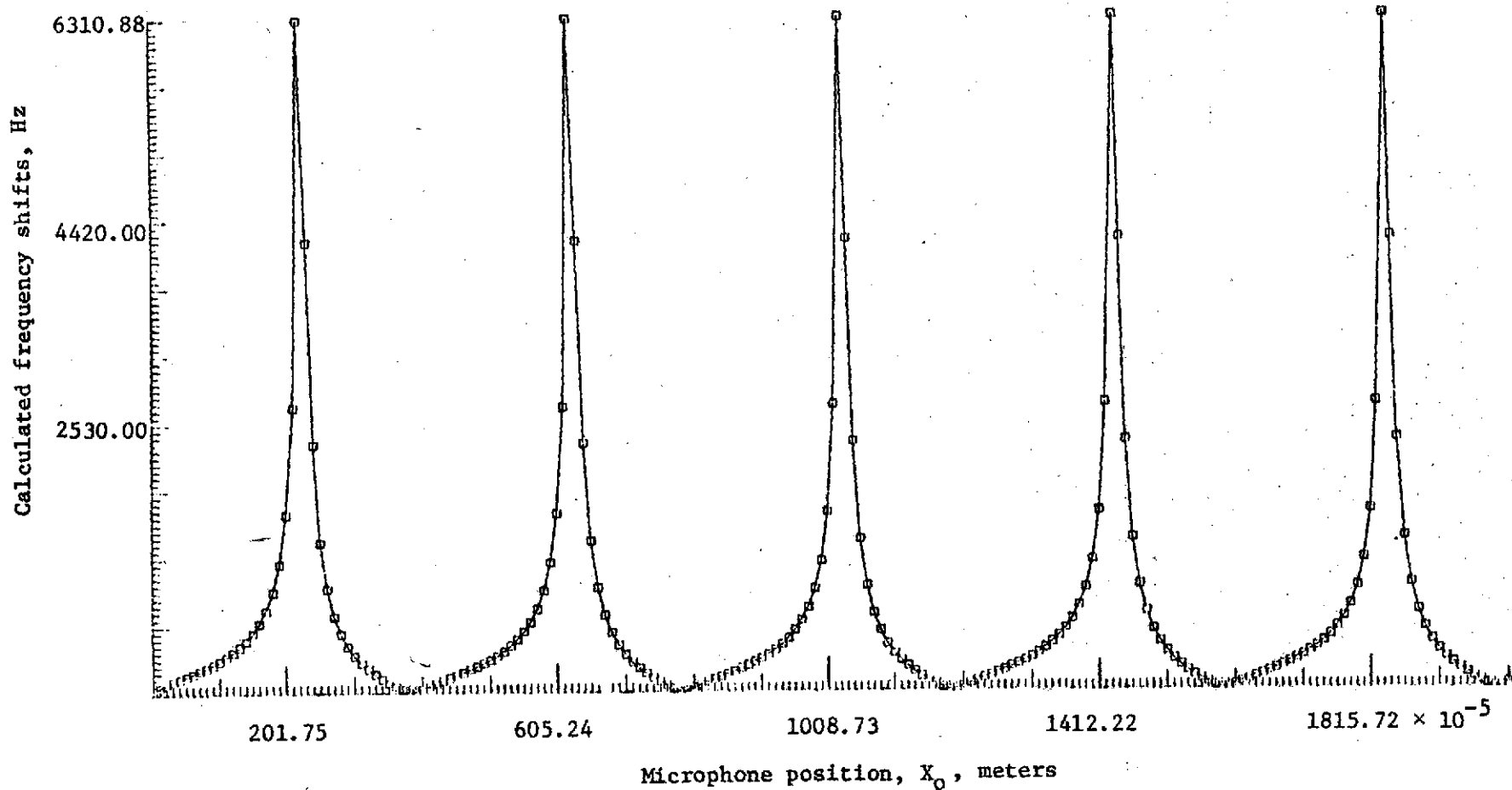


Figure 1.- Calculated frequency shifts as a function of the microphone position with reference to the oscillating surface.

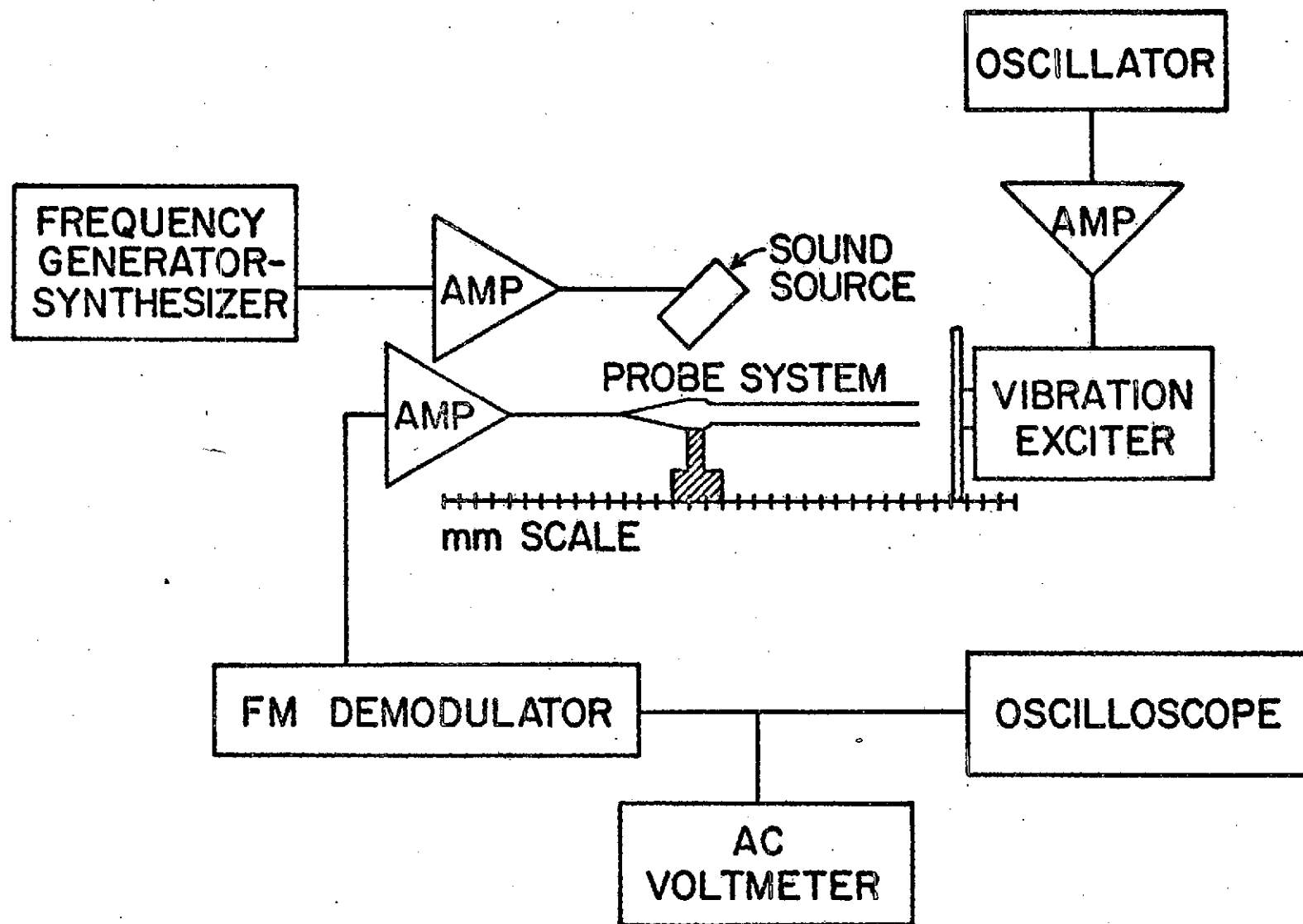


FIGURE 2 - DIAGRAM OF SYSTEM ELECTRONICS

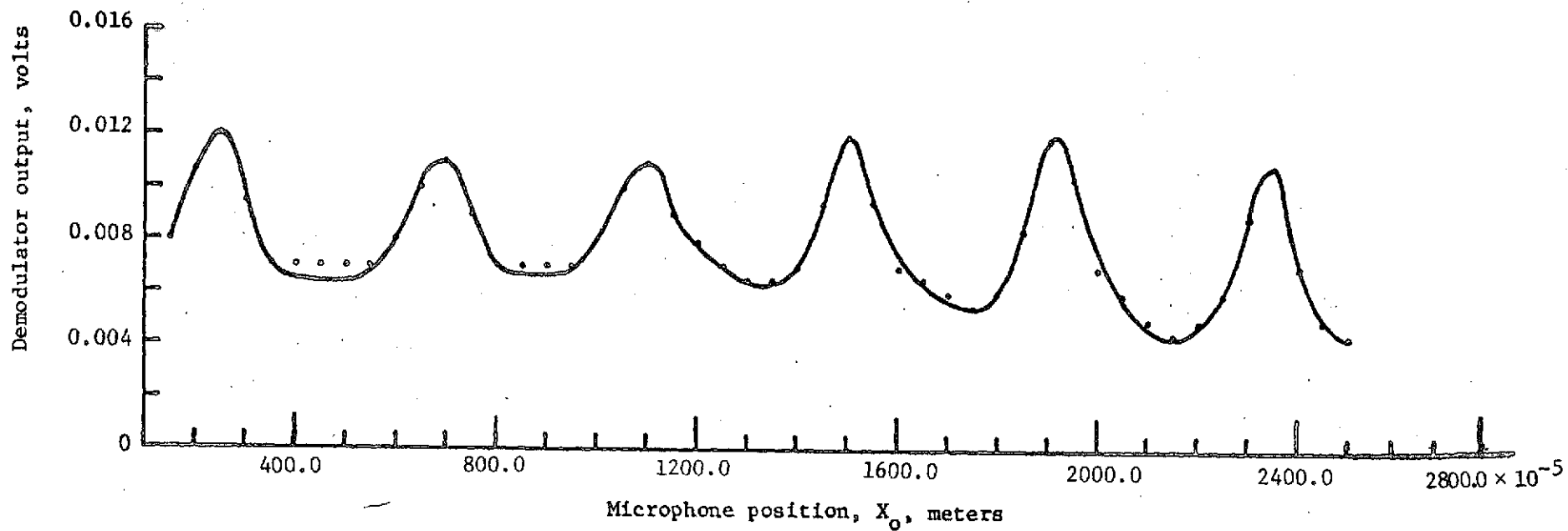


Figure 3.- The demodulator output as a function of microphone distance from the test surface.